Electronic Supplementary Material (ESI) for Journal of Materials Chemistry A
This journal is © The Royal Society of Chemistry 2020

Atomic Ir-doped NiCo layered double hydroxide as bifunctional electrocatalyst for highly efficient and durable water splitting

Supporting Information

Ronglei Fan[a], Qiaoqiao Mu[b], Zhihe Wei[ab], Yang Peng[b] and Mingrong Shen*[a]

[a]*School of Physical Science and Technology, Jiangsu Key Laboratory of Thin Films, Collaborative Innovation Center of Suzhou Nano Science and Technology, Soochow University, 1 Shizi street, Suzhou 215006, China. E-mail: mrshen@suda.edu.cn, Tel: 0086-0512-65112066*

[b]*Soochow Institute of Energy and Material Innovations, College of Energy, Provincial Key Laboratory for Advanced Carbon Materials and Wearable Energy Technologies, Soochow University, Suzhou 215006, China*

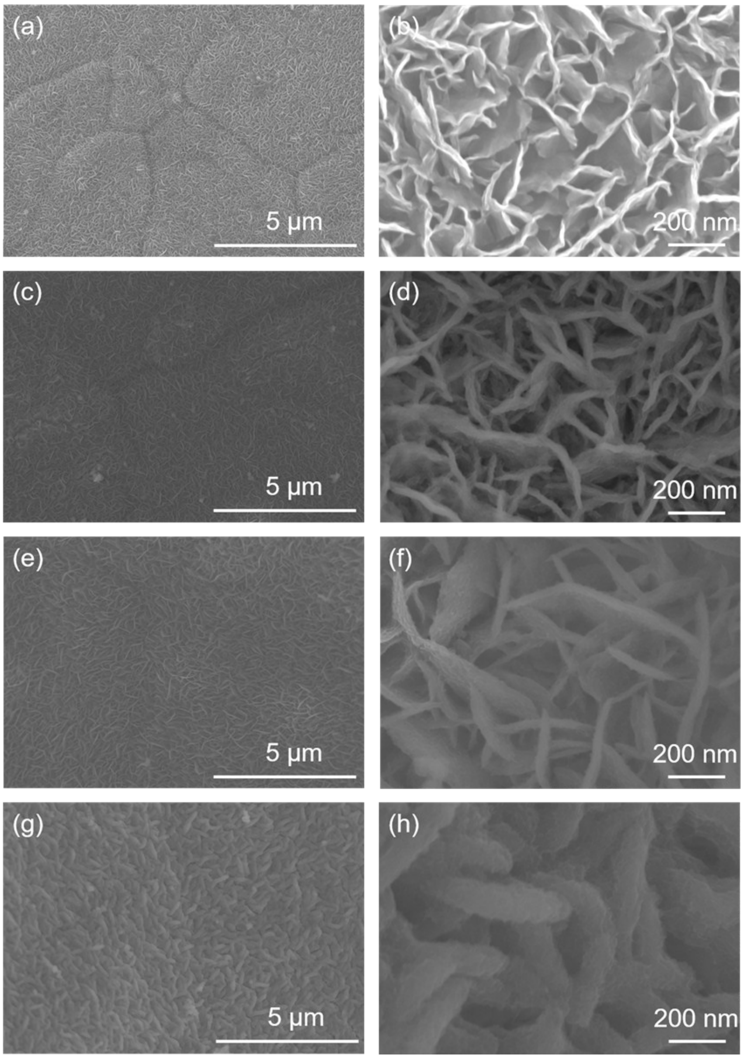

Fig. S1 SEM images of (a, b) the pristine NiCo LDH and Ir-NiCo LDH prepared by adding different amounts of $IrCl_3$ in the Ir precursor: (c, d) 10 μL, (e, f) 25 μL, (g, h) 100 μL.

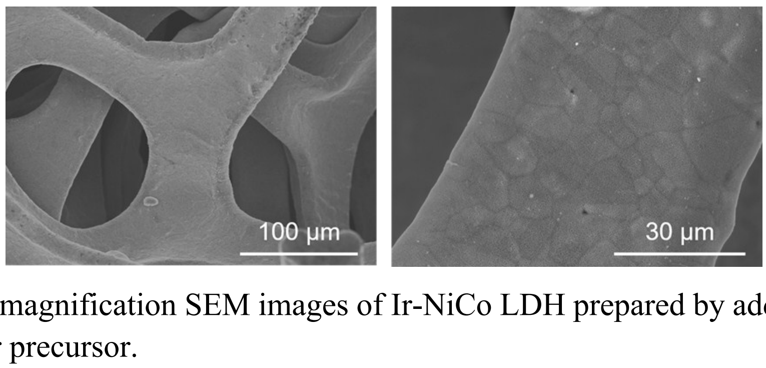

Fig. S2 Low-magnification SEM images of Ir-NiCo LDH prepared by adding 50 μL of $IrCl_3$ in the Ir precursor.

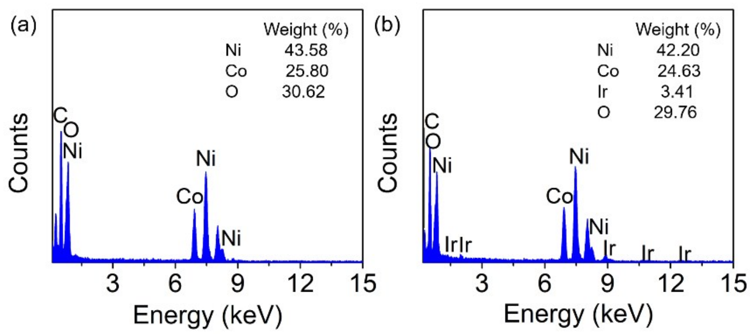

Fig. S3 EDS spectrum and the corresponding element ratios detected in the (a) pristine NiCo LDH and (b) Ir-NiCo LDH.

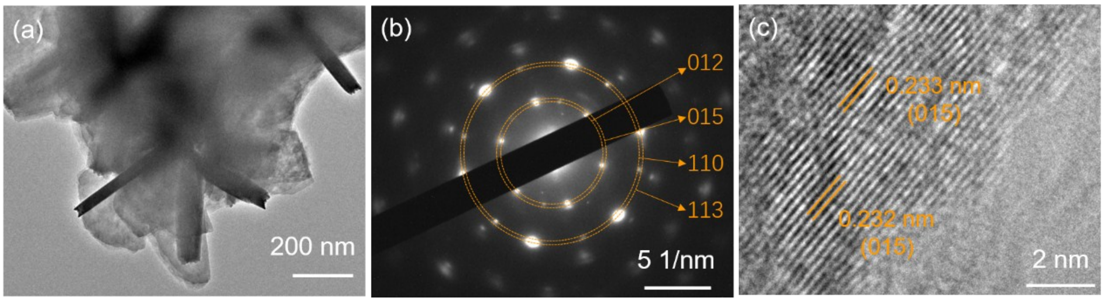

Fig. S4 (a) Low-resolution TEM image, (b) SAED pattern and (c) high-resolution TEM image of the pristine NiCo LDH.

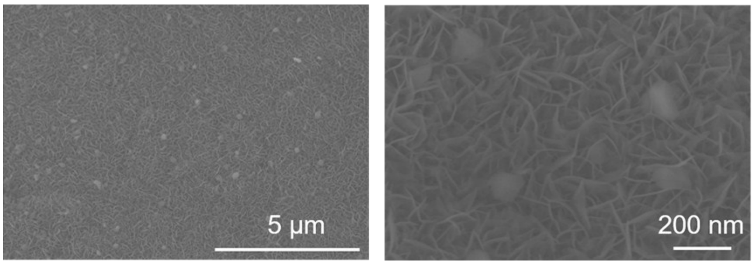

Fig. S5 SEM images of 3.4 wt% of Ir nanoparticles on NiCo LDH.

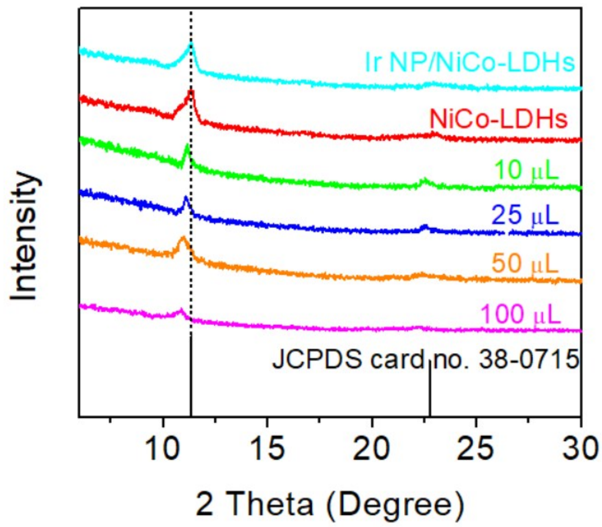

Fig. S6 Enlarged XRD patterns of pristine NiCo LDH, Ir NPs/NiCo LDH and Ir-NiCo LDH with different amounts of Ir content

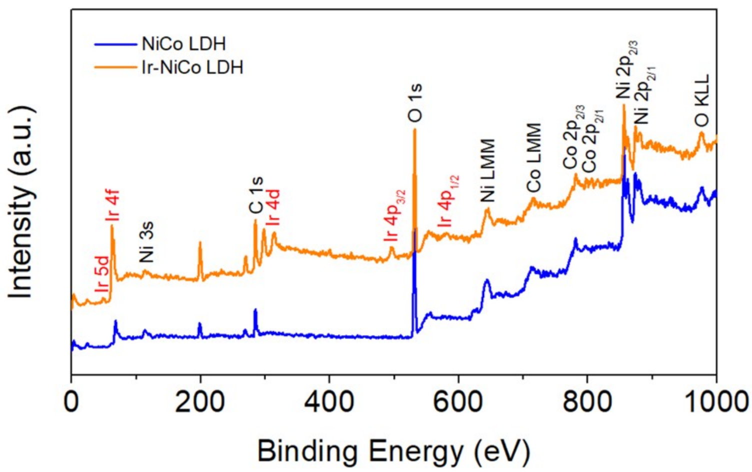

Fig. S7 XPS survey spectra of the pristine NiCo LDH and Ir-NiCo LDH.

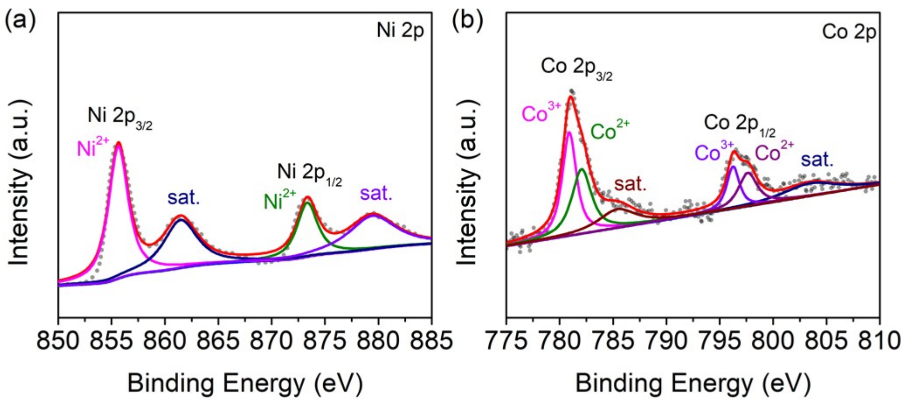

Fig. S8 High-resolution XPS (a) Ni 2p and (b) Co 2p spectra for the pristine NiCo LDH.

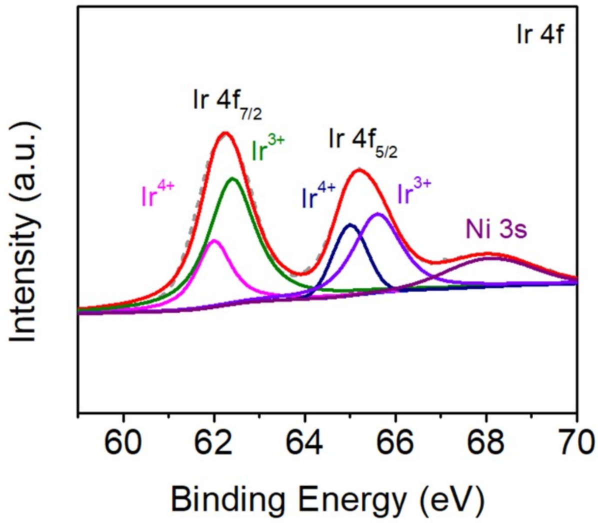

Fig. S9 High-resolution XPS Ir 4f spectrum of Ir-NiCo LDH.

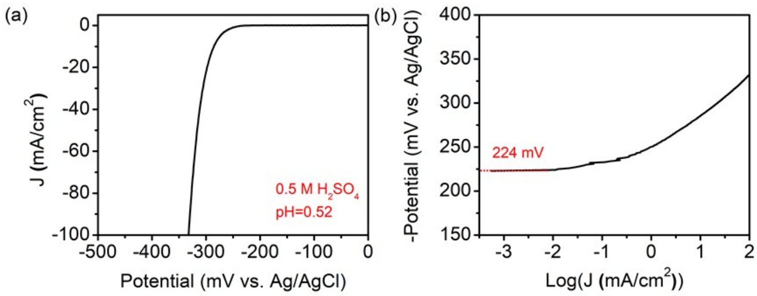

Fig. S10 (a) Polarization curve and (b) corresponding Tafel plot of the Pt sheet in a 0.5 M H_2SO_4 aqueous solution (pH = 0.52). The Ag/AgCl (3M KCl) reference electrode is calibrated to be approximately 0.197 V versus the standard potential (0.197 V_{RHE}).

Two Pt electrodes were first polished and cycled in 0.5 M H_2SO_4 electrolyte at about ±1.8 V versus Ag/AgCl (3M KCl) for 2 hours to remove the surface impurity, and then employed as both working electrode (WE) and counter electrode (CE) in a fresh 0.5 M H_2SO_4 electrolyte. The electrolyte was saturated by hydrogen before use, and continuous H_2 was bubbled over the WE during the calibration.

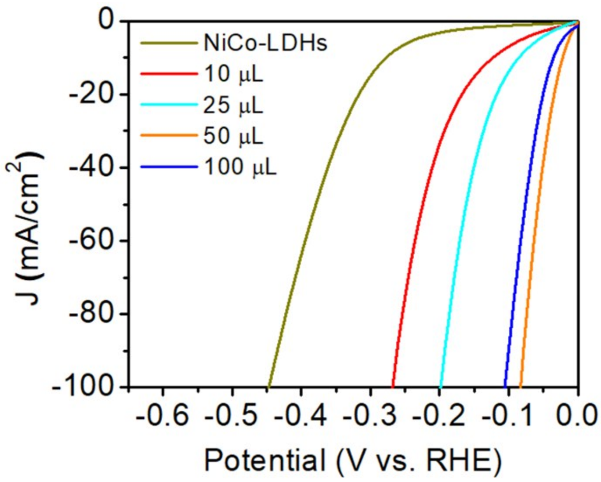

Fig. S11 HER polarization curves of Ir-NiCo LDH samples synthesized with different amounts of $IrCl_3$.

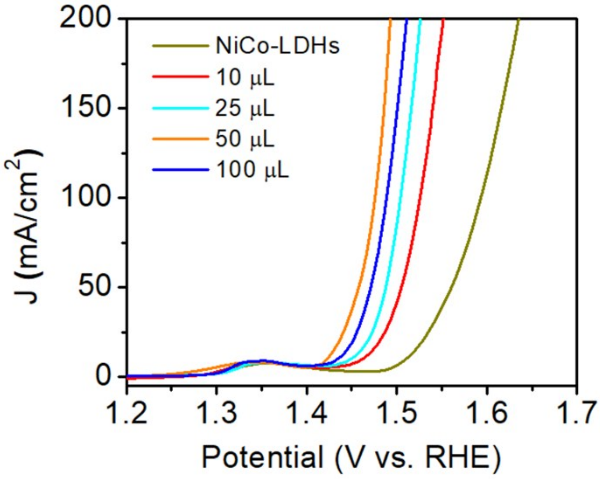

Fig. S12 OER polarization curves of Ir-NiCo LDH samples synthesized with different amounts of $IrCl_3$.

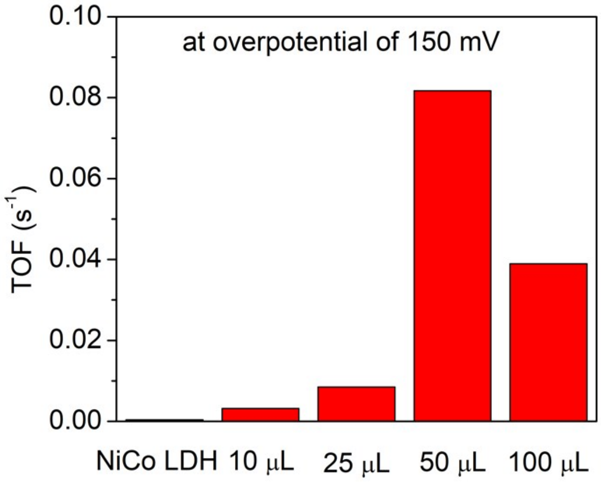

Fig. S13 TOF calculation from HER at the overpotential of 150 mV for Ir-NiCo LDH samples synthesized with different amounts of Ir content.

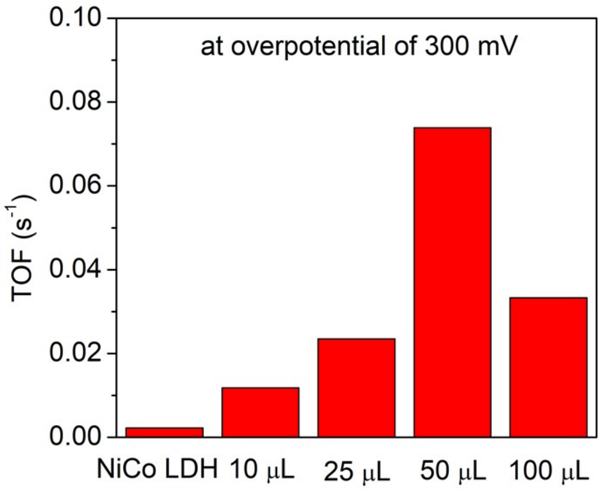

Fig. S14 TOF calculation from OER at the overpotential of 300 mV for Ir-NiCo LDH samples synthesized with different amounts of Ir content.

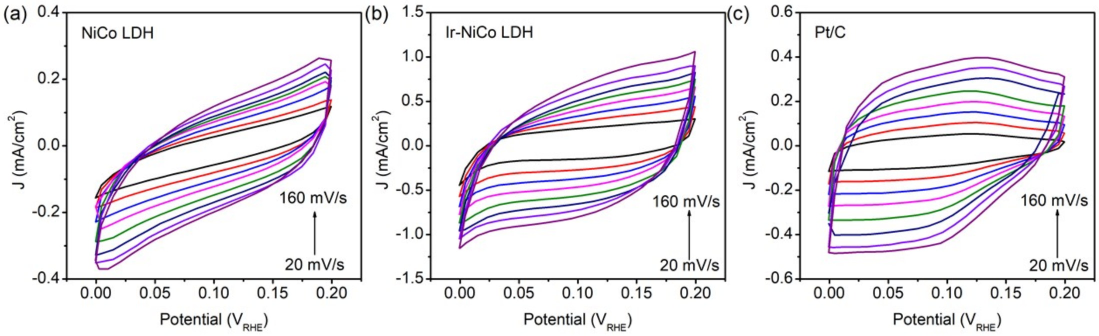

Fig. S15 CV curves in a non-Faradaic potential range (0-0.2 V_{RHE}) of (a) NiCo LDH, (b) Ir-NiCo LDH, (c)Ir/C in N_2-saturated 1.0 M KOH at scan rate of 20 mV/s, 40 mV/s, 60 mV/s, 80 mV/s, 100 mV/s, 120 mV/s, 140 mV/s, 160 mV/s.

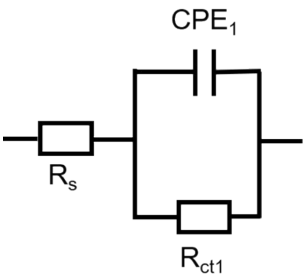

Fig. S16 Equivalent circuit model corresponding to the charge transfer from the NF to the electrolyte through a catalyst. The equivalent circuit elements include a series resistance (R_s) in series with a parallel arrangement of a charge-transfer resistance (R_{ct}) and a constant phase element (CPE_1).

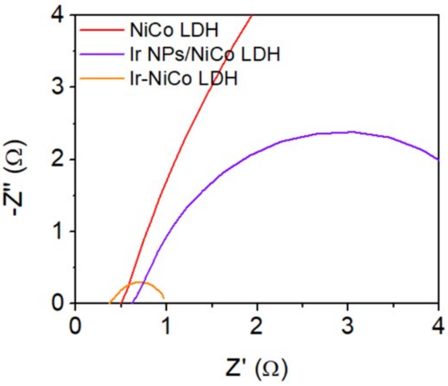

Fig. S17 Nyquist plots of the pristine NiCo LDH, Ir NP NiCo LDH and Ir-NiCo LDH at an overpotential of 270 mV.

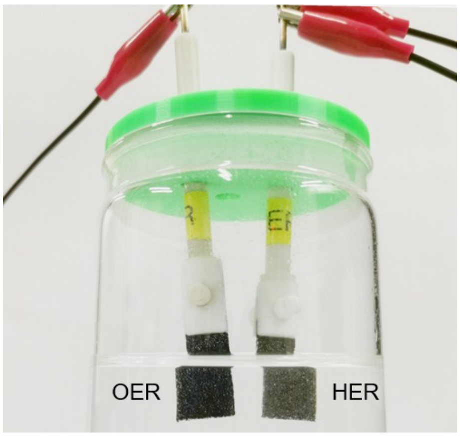

Fig. S18 Optical photograph of overall water splitting performance measured in a two-electrode configuration.

Fig. S19 Optical photograph showing the current of the Ir-NiCo LDH couple driven by a 1.5 V AA battery.

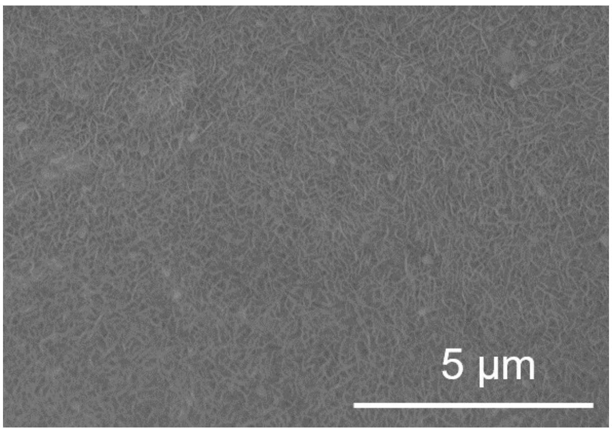

Fig. S20 SEM image of Ir NPs/NiCo LDH after long-term durability test.

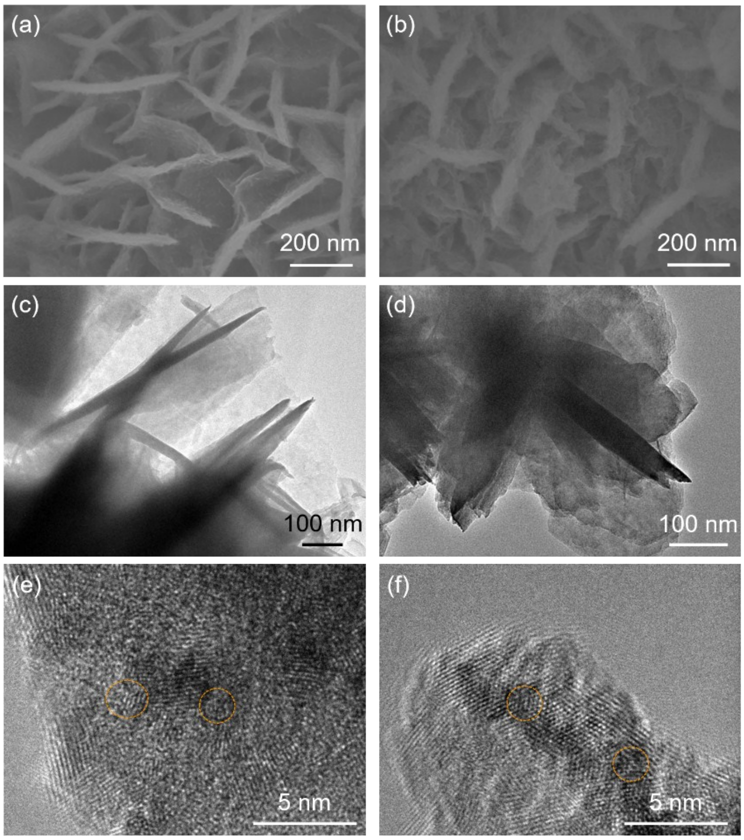

Fig. S21 SEM, TEM and high-resolution TEM images of the Ir-NiCo LDH after 200 h of (a, c, e) HER and (b, d, f) OER stability test. The crystalline phases with lattice distortions in (e) and (f) were noted by orange circles.

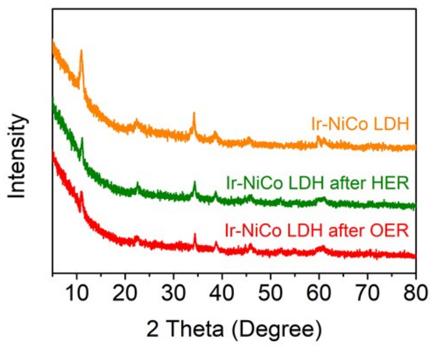

Fig. S22 XRD patterns of the Ir-NiCo LDH after 200 h of HER and OER stability test.

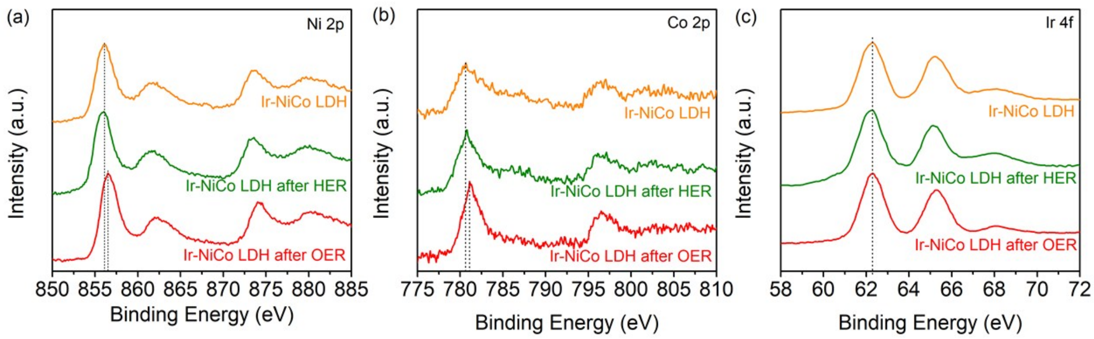

Fig. S23 High-resolution XPS (a) Ni 2p, (b) Co 2p and (c) Ir 4f spectra of the Ir-NiCo LDH after 200 h of HER and OER stability test.

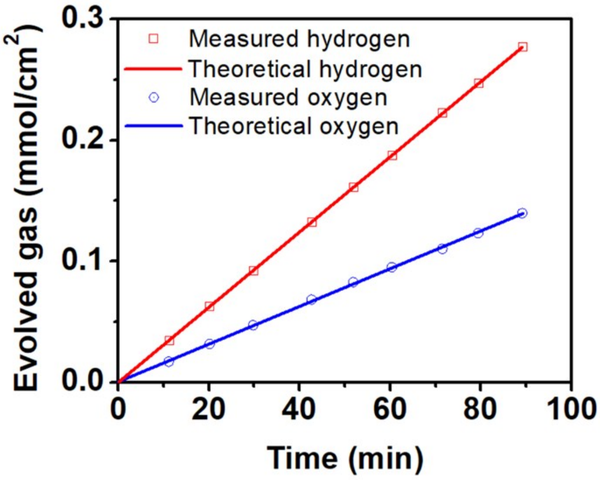

Fig. S24 Amount of gas calculated and experimentally measured along reaction time for overall water splitting of Ir-NiCo LDH at 10 mA/cm^2.

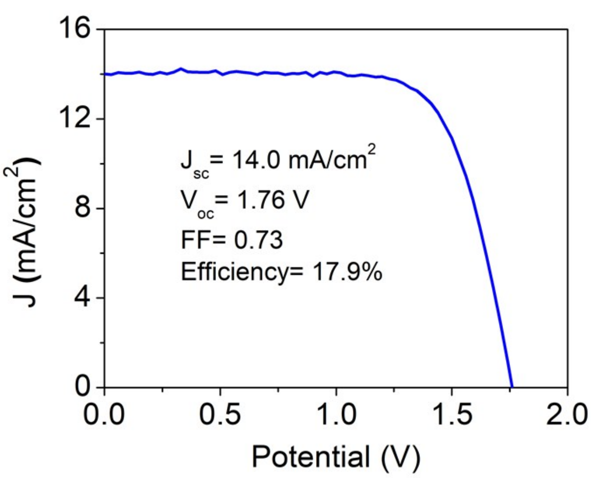

Fig. S25 Polarization curves of three series-connected ordinary solar cells under simulated 1-sun illumination.

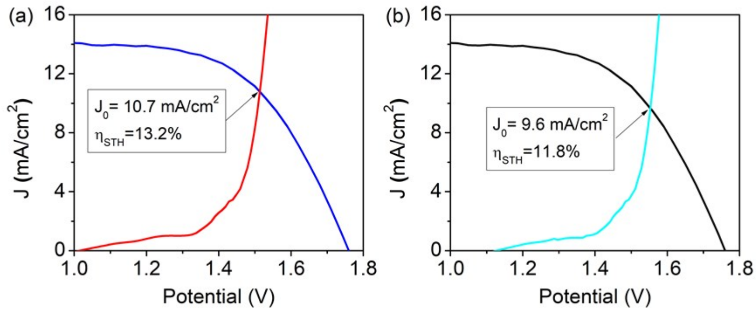

Fig. S26 Polarization curves for overall water splitting using (a) the Pt/C || Ir/C, and (b) Ir NPs/NiCo LDH electrode as both the cathode and anode, and the three series-connected ordinary single crystal Si solar cells.

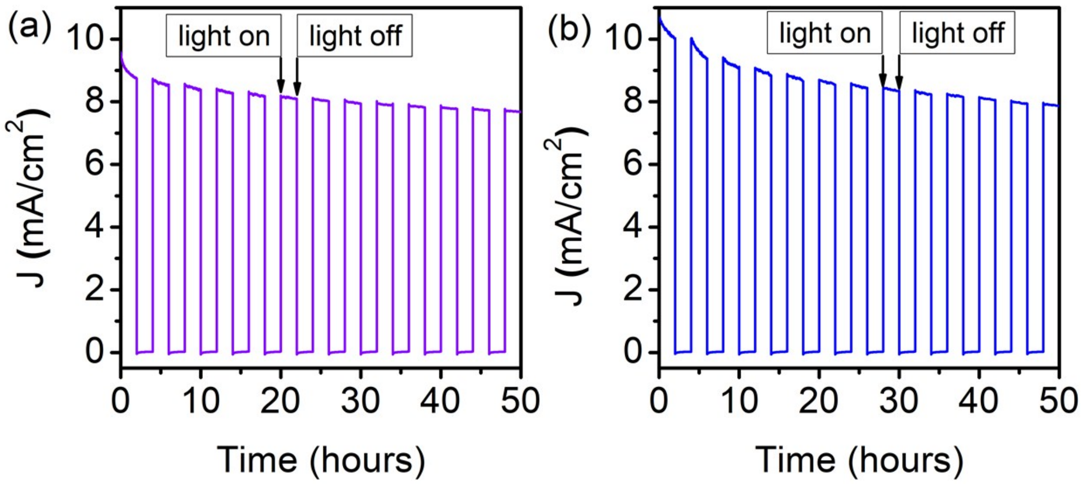

Fig. S27 Time-dependent current output for (a) Ir NPs/NiCo LDH and (b) Pt/C || Ir/C couple under chopped illumination during continuous overall water splitting.

Table S1. Contents of different elements in the Ir precursor solution before and after the spontaneous galvanic displacement reaction.

Ir precursor solution	**Ni (ppm/μmol)**	**Co (ppm/μmol)**	**Ir (ppm/μmol)**
Before galvanic displacement reaction	$0.02/1.4*10^{-2}$	$-0.13/-8.8*10^{-2}$	23.92/5.0
After galvanic displacement reaction	$0.9/6.5*10^{-1}$	1.56/1.1	13.86/2.9

Table S2. The compositions of the pristine NiCo LDH and Ir-NiCo LDH with different amounts of $IrCl_3$ determined by ICP-AES.

Catalyst	Ni (ppm)	Co (ppm)	Ir (ppm)	Atomic ratio of metals (Ni:Co:Ir)	Ir content (wt%)
NiCo LDH	113.82	67.15	-	1.70:1	0
Ir-NiCo LDH (10 μL)	113.68	66.62	2.68	42.42:24.86:1	1.0
Ir-NiCo LDH (25 μL)	113.22	66.35	6.07	18.65:10.93:1	2.3
Ir-NiCo LDH (50 μL)	112.92	65.59	8.91	12.67:7.36:1	3.4
Ir-NiCo LDH (100 μL)	112.33	65.23	17.26	6.51:3.78:1	6.5

Table S3 Summary of HER performances of state-of-the-art electrocatalysts in alkaline solutions.

Catalyst	HER (η_{10}, mV)	Tafel slope (mV/dec)	Electrolyte	Reference
Ir-NiCo LDH	21	33	1.0 M KOH	This Work
Ni_5Co_3Mo-OH	52	59	1.0 M KOH	ACS Energy Lett. 2019, 4, 952−959
$MoS_2/Co_9S_8/Ni_3S_2$	113	85	1.0 M KOH	J. Am. Chem. Soc. 2019, 141, 10417−10430
NiFeOx@NiCu	66	67.8	1.0 M KOH	Adv. Mater. 2019, 31, 1806769
NiCo-nitrides/$NiCo_2O_4$	71	62	1.0 M KOH	Adv. Sci. 2019, 6, 1801829
Ni/Mo2C-NCNFs	143	57.8	1.0 M KOH	Adv. Energy Mater. 2019, 1803185
N-P-Ni	25.8	34	1.0 M KOH	ACS Energy Lett. 2019, 4, 805−810
Ir/MoS_2	44	32	1.0 M KOH	ACS Energy Lett. 2019, 4, 368−374
N-$NiMoO_4/NiS_2$	99	74.2	1.0 M KOH	Adv. Funct. Mater. 2018, 1805298
MoS_2@NiO	406	43	1.0 M KOH	Adv. Funct. Mater. 2018, 1807562
NiFeRu-LDH	29	31	1.0 M KOH	Adv. Mater. 2018, 1706279
FeCoNi-HNTAs	58	37.5	1.0 M KOH	Nat. Commun. 2018, 9, 2452
NFN-MOF	87	35.2	1.0 M KOH	Adv. Energy Mater. 2018, 1801065
Ni-Mo nanosheets	35	45	1.0 M KOH	Small 2017, 13, 1701648
EG/Ni_3Se_2/Co_9S_8	160	83	1.0 M KOH	Nano Lett. 2017, 17, 4202−4209
$NiMo_3S_4$	257	98	0.1 M KOH	Angew. Chem. 2016, 128, 15466 –15471
MoS_2/Ni_3S_2	110	83	1.0 M KOH	Angew. Chem. Int. Ed. 2016, 55, 6702 –6707

Table S4. The fitted value of R_s and R_{ct} during HER for pristine NiCo LDH, Ir NPs/NiCo LDH and Ir-NiCo LDH on NF using the equivalent circuits listed in Fig. S13.

Electrodes	R_s (Ω)	R_{ct} (Ω)	C_1 (F)
NiCo LDH	0.48	15.51	$2.62*10^{-5}$
Ir NPs/NiCo LDH	0.57	2.95	$2.5*10^{-4}$
Ir-NiCo LDH	0.35	0.65	$1.2*10^{-4}$

Table S5 Summary of OER performances of state-of-the-art electrocatalysts in alkaline solutions.

Catalyst	HER (η_{10}, mV)	Tafel slope (mV/dec)	Electrolyte	Reference
Ir-NiCo LDH	192	41.2	1.0 M KOH	This Work
NiFe-LDH@NiCu	218	56.9	1.0 M KOH	Adv. Mater. 2019, 31, 1806769
Fe-Doped β-Ni(OH)$_2$	219	53	1.0 M KOH	ACS Energy Lett. 2019, 4, 622−628
NiVIr LDH	203	55.3	1.0 M KOH	ACS Energy Lett. 2019, 4, 1823−1829
Ni_3S_2/MnS	228	41	1.0 M KOH	Applied Catalysis B: Environmental 257 (2019) 117899
FeOOH(Se)	287	54	1.0 M KOH	J. Am. Chem. Soc. 2019, 1411, 77005-7013
Ru/CoFe-LDH	198	39	1.0 M KOH	Nat. Commun. 2019, 10, 1711
Ni/Mo_2C-NCNFs	288	78.4	1.0 M KOH	Adv. Energy Mater. 2019, 1803185
$Ni_3Fe_{0.5}V_{0.5}$ LDH	264	39	1.0 M KOH	Nat. Commun. 2018, 9, 2885
NiFeCr LDH	~ 200	69	1.0 M KOH	Adv. Energy Mater. 2018, 1703189
NiFeV LDH	195	42	1.0 M KOH	Adv. Energy Mater. 2018, 1703341
Co-Mo_2C NPs	347	38	1.0 M KOH	Applied Catalysis B: Environmental 2018, 227, 340–348
MoS_2−Ni_3S_2 HNRs	249	57	1.0 M KOH	ACS Catal. 2017, 7, 2357−2366
P-Co_3O_4	280	51.6	1.0 M KOH	Energy Environ. Sci., 2017, 10, 2563–2569
NiCoFe LDH	275	85	0.10 M KOH	J. Mater. Chem. A, 2016,4, 7245−7250
NiCo LDH nanostructures	367	40	1.0 M KOH	Nano Lett. 2015, 15, 1421−1427
NiFe-LDH	224	52.8	1.0 M KOH	Chem. Sci., 2015, 6, 6624–6631

Table S6. The fitted value of R_s and R_{ct} during OER for pristine NiCo LDH, Ir NPs/NiCo LDH and Ir-NiCo LDH on NF using the equivalent circuits listed in Fig. S13.

Electrodes	R_s (Ω)	R_{ct} (Ω)	C_1 (F)
NiCo LDH	0.61	20.38	$1.7*10^{-5}$
Ir NPs/NiCo LDH	0.71	4.55	$1.1*10^{-4}$
Ir-NiCo LDH	0.41	0.57	$2.0*10^{-4}$

Table. S7 Comparisons of overall water splitting performance for various bifunctional catalysts.

Catalysts	**Electrolytes**	**Potential at 10 mA/cm^2 (V)**	**Reference**
Ir-NiCo LDH	1 M KOH	1.45	This work
Ir NPs/NiCo LDH	1 M KOH	1.51	This work
Pt/C || Ir/C	1 M KOH	1.55	This work
Co-RuIr alloy	0.1 M $HClO_4$	1.52	Adv. Mater. 2019, 31, 1900510
Ir-Doped $NiV(OH)_2$/NF	1.0 M KOH	1.49	ACS Energy Lett. 2019, 4, 1823−1829
Ni_3S_2/MnS/NF	1.0 M KOH	1.54	Applied Catalysis B: Environmental, 2019, 257, 117899
Ni/Mo_2C-nitrogen-doped carbon nanofibers	1 M KOH	1.64	Adv. Energy Mater. 2019, 1803185
NiCo-nitrides/$NiCo_2O_4$/GF	1.0 M KOH	1.68 (at 20 mA cm^2)	Adv. Sci. 2019, 6, 1801829
Co–Fe oxyphosphide microtubes	1.0 M KOH	1.69	Adv. Sci. 2019, 6, 1900576
NiFeRu-LDH/NF	1.0 M KOH	1.52	Adv. Mater. 2018, 30, 1706279
iron fluoride-oxide nanoporous film	1.0 M KOH	1.58	Nat. Comm., 2018, 9, 1809
Co_1Mn_1 carbonate hydroxide/NF	1 M KOH	1.68	J. Am. Chem. Soc., 2017, 139, 8320
Cu@NiFe LDH	1 M KOH	1.54	Energ. Environ. Sci. 10, 2017 1820-1827
N-Ni_3S_2/NF	1 M KOH	1.48	Adv. Mater., 2017, 29, 1701584
$NiCo_2O_4$	1 M NaOH	1.65	Angew. Chem. Int. Ed., 2016, 55, 6290
MoS_2/Ni_3S_2/NF	1 M KOH	1.56	Angew. Chem., 2016, 55, 6702
NiSe/NF	1 M KOH	1.63	Angew. Chem. 2015, 127, 9483
Ni_2P/NF	1 M KOH	1.63	Energy Environ. Sci., 2015, 8, 2347

Table S8. Comparison of overall solar-to-hydrogen conversion efficiency in recent reports and this work

Electrochemical cell	**Solar cell**	**Solar-tohydrogen conversion efficiency**	**Electrolytes**	**Reference**
Ir-NiCo LDH	three series-connected ordinary solar cells	14.8%	1 M KOH	This work
Ir NPs/NiCo LDH	three series-connected ordinary solar cells	13.2	1 M KOH	This work
Pt/C || Ir/C	three series-connected ordinary solar cells	11.8	1 M KOH	This work
Pt || IrO_x	three series-connected Si heterojunction cells	14.2%	1 M KOH	J. Electrochem. Soc., 2016, 163, F1177
Ni-Co-S/Ni-Co-P	three series-connected ordinary solar cells	10.8%	1 M NaOH	J. Mater. Chem. A, 2018, 6, 20297–20303
NiFe inverse opal	four series-connected Si heterojunction cells	9.54%	1 M NaOH	Nano Energy 2017, 42, 1-7
CuCoO nanowires	a commercial planar silicon photovoltaic	4.5%	1 M KOH	Adv. Funct. Mater., 2016, 26, 8555
Co-Bi-NiMoZn	a-Si 3jn (wired device)	4.7%	0.5 M KBi (pH 9.2)	Science, 2011, 334, 645